Progress In Electromagnetics Research M, Vol. 99, 191–200, 2021

AE-STAP Algorithm for Space-Time Anti-Jamming

Ruiyan Du[1, 2, *], Fulai Liu[1, 2], Xiaodan Chen[1, *], and Jiaqi Yang[1]

Abstract—Space-time adaptive processing (STAP) algorithms can provide effective interference suppression potential in global navigation satellite system (GNSS). However, the performance of these algorithms is limited by the training samples support in practical applications. This paper presents an effective STAP based on atoms extension (named as AE-STAP) algorithm to provide better anti-jamming performance even if within a very small number of snapshots. In the proposed algorithm, a spatial-temporal plane is constructed firstly by the sparsity of received signals in the spatial domain. In the plane, each grid point corresponds to a space-time steering vector, named as an atom. Then, the optimal atoms are selected by searching atoms that best match with the received signals in the spatial-temporal plane. These space-time steering vectors corresponding to the optimal atoms are used to construct the interference subspace iteratively. Finally, in order to improve the estimation accuracy of interference subspace, an atoms extension (AE) method is given by extending the optimal atoms in a diagonal manner. The STAP weight vector is obtained by projecting the snapshots on the subspace orthogonal to the interference subspace. Simulation results demonstrate that the proposed method can provide better interference suppression performance and higher output signal-to-interference-plus-noise ratios (SINRs) than the previous works.

1. INTRODUCTION

Space-time adaptive processing (STAP) is a critical technique for global navigation satellite system (GNSS) to suppress the influence of multipath signals, radio frequency interference (RFI), etc. [1,2]. It is known that the full-dimension (FD) STAP algorithm requires at least two times of the degrees of freedom (DoFs) in independent and identically distributed (IID) samples to achieve a signal-to-interference-plus-noise ratio (SINR) loss within 3 dB, which is usually impractical for heterogenous environments, especially with large arrays [3]. Furthermore, high computational complexity and storage space are needed to compute the FD STAP filter. Therefore, STAP algorithms with attractive performance at low sample support and low computational complexity are of great importance in practical applications. To deal with such issues, numerous STAP algorithms have been proposed in the last decades. Reduced-dimension (RD) STAP algorithms, such as the multiple Doppler channels joint processing scheme (mDT) [4], joint-domain localized algorithm (JDL) [5], space-time multiple beam (STMB) algorithm [6], and robust two-stage RD SA-STAP considering inaccurate prior knowledge (RTSKA-RD-SA-STAP) [7] are proposed by employing a low dimension for reducing the computational complexity and sample support requirements. These algorithms have limited steady-state performance due to reduced system DoFs. In this context, reduced-rank STAP algorithms, such as the principle components (PC) [8], cross-spectral metric (CSM) [9], and multistage Wiener filter (MSWF) [10], can provide high steady-state performance by using two times of the clutter rank of IID samples. However, the advantage of these algorithms comes at the expense of reduced system DoFs. Recently, knowledge-aided STAP algorithms

Received 14 September 2020, Accepted 15 October 2020, Scheduled 15 December 2020

* Corresponding author: Ruiyan Du (ruiyandu@126.com), Xiaodan Chen (cxddxc@163.com).

[1] Engineer Optimization & Smart Antenna Institute, Northeastern University at Qinhuangdao, Qinhuangdao, China. [2] School of Computer Science and Engineering, Northeastern University, Shenyang, China.

have shown improved performance with a small number of training samples by exploiting prior knowledge of environments or radar systems [11]. However, these algorithms suffer from performance degradation in the presence of prior knowledge errors.

Owing to the successful application of compressive sensing (CS) in the parameter estimation, the attention has been focused on STAP based on sparse recovery (SR-STAP) techniques by exploiting the sparsity of the jamming signals [12,13]. Although SR-STAP algorithms show tremendous advantages in the case of minimal training samples as compared to conventional STAP ones, their disadvantages should not be ignored. It should be noted that the conventional SR-STAP is implemented under the condition that the jamming signal is matched with the spatial-temporal grids, i.e., the spatial-temporal plane is divided into a large number of grids where the jamming patches are assumed to exactly lie on some of the grids. However, when the actual jamming signal is mismatched with the spatial-temporal grids, the performance of conventional SR-STAP will decrease significantly. This phenomenon is known as the off-grid problem in SR-STAP. The off-grid in the SR-STAP is a special form of the usual off-grid in CS. It is easy to design a compact over-complete STAP dictionary to mitigate the off-grid issue. However, a dense grid set not only increases the correlation between two adjacent spatial-temporal steering vectors but also gives rise to the computational load [14], which restricts its practical application. Some researchers have focused on the off-grid cases in the direction of arrival (DOA) estimation, where the DOAs of interest may not exactly lie on the grids [15, 16]. An efficient root sparse Bayesian learning (SBL) method is proposed to speed up the off-grid SBL method [15]. To solve the nonuniformity of the noise variance and off-grid error, SBL based method of off-grid DOA estimation under nonuniform noise is proposed in [16]. However, it is difficult to apply the first-order approximation method to off-grid SR-STAP. A parameter-searched orthogonal matching pursuit (PSOMP) algorithm is proposed to eliminate the basis mismatch in SR-STAP, which has a better performance and lower computational complexity than orthogonal matching pursuit (OMP) algorithm [17]. However, the optimization problem in PSOMP is not easy to solve.

In this paper, an STAP based on atoms extension (AE-STAP) algorithm is proposed to solve the off-grid problem of SR-STAP, which can effectively select more appropriate atoms that are matched with jamming signals. The proposed algorithm can mitigate the influence of off-grid in SR-STAP and also can efficiently improve the performance of SR-STAP in limited-training-sample scenarios. The paper is organized as follows. Section 2 outlines the signal model of STAP. Section 3 introduces the proposed AE-STAP algorithm. Simulations are carried out to demonstrate the performance of our algorithm in Section 4. Finally, the conclusion is summarized in Section 5.

Notation: $(\cdot)^{\mathrm{T}}$, $(\cdot)^{\mathrm{H}}$, and $(\cdot)^{-1}$ denote the transpose operation, Hermitian transpose operation, and matrix inverse, respectively. $\otimes$ represents the Kronecker product. $\mathbb{C}$ expresses the complex field. Moreover, $\|\cdot\|_0$, $\|\cdot\|_2$, and $\|\cdot\|_F$ stand for l_0 norm, l_2 norm, and Frobenius norm, respectively. $\varnothing$ stands for empty set. $\mathbf{E}(\cdot)$ indicates the statistical average operation.

2. DATE MODEL

Consider an STAP model with a uniform linear array (ULA) consisting of M elements equispaced by d, as shown in Fig. 1. Each element in the ULA is equally spaced with N taps. The $MN \times 1$ space-time observation vector $\boldsymbol{x}(t) = [x_{11}(t), x_{12}(t), \ldots, x_{1N}(t), x_{21}(t), \ldots, x_{2N}(t), \ldots, x_{MN}(t)]^{\mathrm{T}}$ at time t can be expressed as

$$\boldsymbol{x}(t) = \boldsymbol{a}(\theta_s, f_s)\boldsymbol{s}_1(t) + \sum_{l=1}^{L} \boldsymbol{a}(\theta_l, f_l)\boldsymbol{j_l}(t) + \boldsymbol{n}(t) = \boldsymbol{A}\boldsymbol{s}(t) + \boldsymbol{n}(t) \tag{1}$$

where θ_s and $\theta_l (l = 1, 2, \ldots, L)$ denote the DOAs of the desired signal and L interference signals, respectively. f_s and f_l $(l = 1, 2, \ldots, L)$ are normalized frequencies of the desired signal and L interference signals, respectively. $\boldsymbol{s}(t) = [s_1(t), j_1(t), \ldots, j_l(t)]^{\mathrm{T}}$ with $s_1(t)$ denoting the desired signal and $j_l(t)$ $(l = 1, 2, \ldots, L)$ the interference signals, respectively. The noise vector $\boldsymbol{n}(t) = [n_{11}(t), n_{12}(t), \ldots, n_{1N}(t), \ldots n_{21}(t), \ldots, n_{MN}(t)]^{\mathrm{T}}$ with $n_{mn}(t)$ $(m = 1, 2, \ldots, M, n = 1, 2, \ldots, N)$ standing for the additive noise. The $MN \times 1$ spatial-temporal steering vector $\boldsymbol{a}(\theta, f)$ stands for the array response with regard to the signal where DOA θ and f denote the DOA and normalized

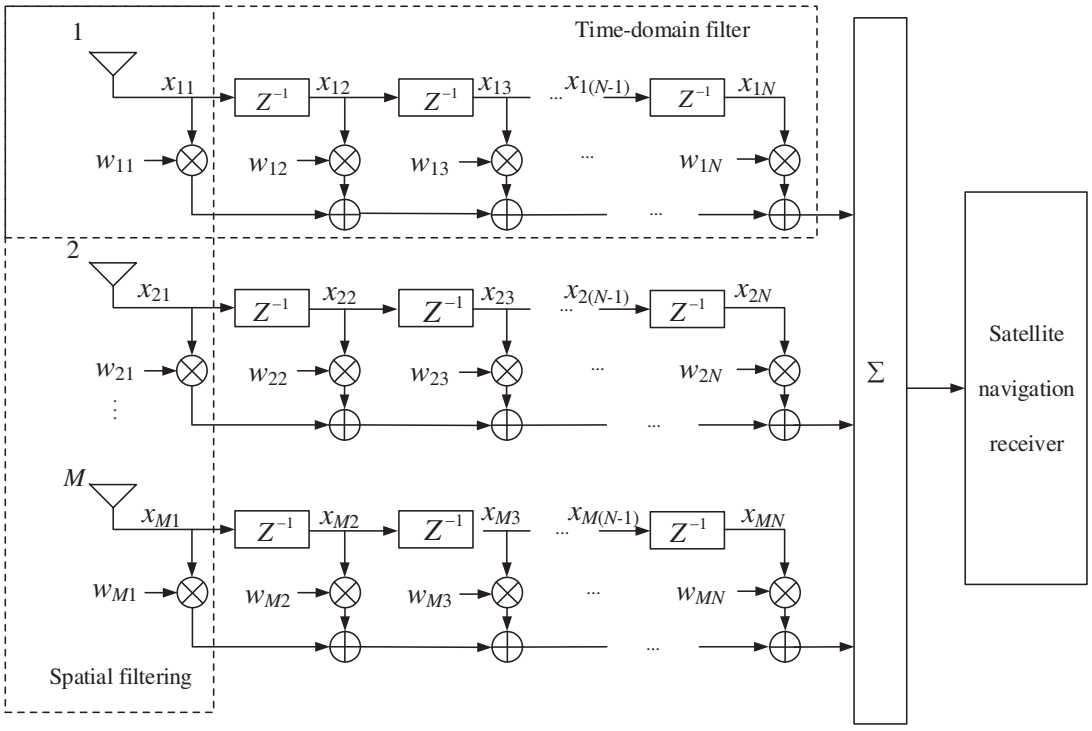

Figure 1. STAP model.

frequency, respectively. The array manifold matrix $\boldsymbol{A} = [\boldsymbol{a}(\theta_s, f_s), \boldsymbol{a}(\theta_1, f_1), \ldots, \boldsymbol{a}(\theta_L, f_L)]$. The space-time steering vector $\boldsymbol{a}(\theta, f)$ is given by $\boldsymbol{a}(\theta, f) = \boldsymbol{a}_s(\theta) \otimes \boldsymbol{a}_t(f)$. $\boldsymbol{a}_s$ and $\boldsymbol{a}_t(f)$ can be written as

$$\boldsymbol{a}_s(\theta) = \left[1, e^{-j2\pi d \sin(\theta)/\lambda}, \ldots, e^{-j2\pi d(M-1)\sin(\theta)/\lambda}\right]^{\mathrm{T}} \tag{2}$$

$$\boldsymbol{a}_t(f) = \left[1, e^{-j2\pi f T_s}, \ldots, e^{-j2\pi(N-1)fT_s}\right]^{\mathrm{T}} \tag{3}$$

where $\boldsymbol{a}_s$ and $\boldsymbol{a}_t(f)$ are the spatial steering vector and temporal steering vector, respectively. T_s represents the delay time of each tap.

Further, the STAP filter output $y(t)$ at time t can be written as

$$y(t) = \boldsymbol{w}^{\mathrm{H}} \boldsymbol{x}(t) \tag{4}$$

where the $MN \times 1$ complex-valued weight vector $\boldsymbol{w} = [w_{11}, w_{12}, \ldots, w_{1N}, w_{21}, \ldots, w_{2N}, \ldots, w_{MN}]^{\mathrm{T}}$ with w_{mn} $(m = 1, 2, \ldots, M,\ n = 1, 2, \ldots, N)$ being the spatial-temporal weight for the nth tap on the mth antenna.

3. ALGORITHM FORMULATION

In this section, the proposed algorithm will be introduced in detail. Firstly, the received signals are represented sparsely in Subsection 3.1. In Subsection 3.2, the received signals are sparse restored to obtain the optimal atoms in the space-time dictionary, and then the optimal atoms are extended. Finally, the space-time optimal weight vector is solved in Subsection 3.3.

3.1. Sparse Representation of the Received Signal

The desired signals are submerged below the noise, and the power of narrow-band compression interference signal is above 20 dB of the noise. The number of interference signals is much smaller

than the DoF of space-time two-dimensional processing. Therefore, the received signals are sparse in space-time spectrum. In this subsection, the sparse representation of the received signals is given.

The entire normalized spatial-Doppler plane is uniformly discretized into $N_s = \rho_s \times M$ and $N_f = \rho_f \times N$ grid points along the space and time axes, where $\rho_s,\ \rho_f \gg 1$ denote the resolution scales of the discretized plane. Each grid point corresponds to a space-time steering vector. The $MN \times N_s N_f$ matrix $\boldsymbol{\Phi}$ is the overcomplete STAP dictionary, as given by

$$\boldsymbol{\Phi} = \left[\boldsymbol{a}(\theta_{11}, f_{11}), \ldots, \boldsymbol{a}(\theta_{1N_f}, f_{1N_f}), \ldots, \boldsymbol{a}(\theta_{N_s N_f}, f_{N_s N_f})\right] \tag{5}$$

where θ_{ij} and f_{ij} $(i = 1, 2, \ldots, N_s, j = 1, 2, \ldots, N_f)$ denote the quantised elevation angles and quantised Doppler frequencies, respectively. The spatial-temporal steering vectors $\boldsymbol{a}(\theta_{ij}, f_{ij})$ $(i = 1, 2, \ldots, N_s, j = 1, 2, \ldots, N_f)$ are called atoms in the overcomplete STAP dictionary.

Assume that all the interference signals lie exactly on some of the grids, and then the model in Eq. (1) can be rewritten as

$$\boldsymbol{x}(t) = \boldsymbol{\Phi}\boldsymbol{\gamma} + \boldsymbol{n}(t) \tag{6}$$

where $\boldsymbol{\gamma} \in \mathbb{C}^{N_s N_f \times 1}$ is the sparse signal with the non-zero elements representing the locations of interference signals.

The problem in Eq. (6) is the canonical signal for the SR problem, which can be interpreted as estimating a sparse vector $\boldsymbol{\gamma}$ from the received signal $\boldsymbol{x}(t)$. Specifically, $\boldsymbol{\gamma}$ could be formulated as the following minimal optimisation problem

$$\min_{\boldsymbol{\gamma}} \|\boldsymbol{\gamma}\|_0 \quad s.t.\ \|\boldsymbol{x} - \boldsymbol{\Phi}\boldsymbol{\gamma}\|_2^2 \le \varepsilon \tag{7}$$

where the l_0 norm measures the number of non-zero elements in a vector; $\|.\|_2$ stands for the l_2 norm; and ε is the noise error allowance.

3.2. Extension of the Optimal Atoms

Although the problem in Eq. (7) has been shown to be NP-hard problem, many low complexity algorithms have been proposed, and one of them, known as orthogonal matching pursuit (OMP) algorithm [18], is selected in this paper. In each iteration, the optimal atoms are calculated by the maximum correlation between the received signals and atoms in the STAP dictionary $\boldsymbol{\Phi}$. The indices of atoms in $\boldsymbol{\Phi}$ are recorded as λ_i $(i = 1, 2, \ldots, L)$. After sparse recovery processing by OMP algorithm, the angles and frequencies of interference signals can be estimated by the optimal atomic matrix $\widetilde{\boldsymbol{\Phi}}$.

In practice, there is always a bias between the interference signals and the discrete grids. No matter how dense we divide the spatial-temporal plane, the bias always exists. In order to reduce the estimation bias of the optimal atomic matrix $\widetilde{\boldsymbol{\Phi}}$, the angles and frequencies of the estimated interference signals need to be extended. Therefore, two atoms extension (AE) methods are considered. The first AE method extends the optimal atoms along the angle and frequency axis. The second one extends the optimal atoms in a diagonal manner. Taking the kth optimal atom $\boldsymbol{a}(\theta_{\lambda_k}, f_{\lambda_k})$ in $\widetilde{\boldsymbol{\Phi}}$ as an example, two forms of AE methods are considered, as shown in Fig. 2 and Fig. 3, respectively.

As shown in Fig. 2 and Fig. 3, the atomic cluster $\widetilde{\boldsymbol{u}}_{k1}$ and $\widetilde{\boldsymbol{u}}_{k2}$ with the center of atom $\boldsymbol{a}(\theta_{\lambda_k}, f_{\lambda_k})$ can be written as

$$\begin{aligned}\widetilde{\boldsymbol{u}}_{k1} = [&\widetilde{\boldsymbol{a}}(\theta_{\lambda_k} - \Delta\theta, f_{\lambda_k} + \Delta f), \widetilde{\boldsymbol{a}}(\theta_{\lambda_k} - \Delta\theta, f_{\lambda_k}), \widetilde{\boldsymbol{a}}(\theta_{\lambda_k} - \Delta\theta, f_{\lambda_k} - \Delta f),\\ &\widetilde{\boldsymbol{a}}(\theta_{\lambda_k}, f_{\lambda_k} + \Delta f), \boldsymbol{a}(\theta_{\lambda_k}, f_{\lambda_k}), \widetilde{\boldsymbol{a}}(\theta_{\lambda_k}, f_{\lambda_k} - \Delta f),\\ &\widetilde{\boldsymbol{a}}(\theta_{\lambda_k} + \Delta\theta, f_{\lambda_k} + \Delta f), \widetilde{\boldsymbol{a}}(\theta_{\lambda_k} + \Delta\theta, f_{\lambda_k}), \widetilde{\boldsymbol{a}}(\theta_{\lambda_k} + \Delta\theta, f_{\lambda_k} - \Delta f)]\end{aligned} \tag{8}$$

$$\begin{aligned}\widetilde{\boldsymbol{u}}_{k2} = [&\widetilde{\boldsymbol{a}}(\theta_{\lambda_k} - \Delta\theta, f_{\lambda_k} + \Delta f), \widetilde{\boldsymbol{a}}(\theta_{\lambda_k} - \Delta\theta, f_{\lambda_k} - \Delta f), \boldsymbol{a}(\theta_{\lambda_k}\ f_{\lambda_k}),\\ &\widetilde{\boldsymbol{a}}(\theta_{\lambda_k} + \Delta\theta, f_{\lambda_k} + \Delta f), \widetilde{\boldsymbol{a}}(\theta_{\lambda_k} + \Delta\theta, f_{\lambda_k} - \Delta f)]\end{aligned} \tag{9}$$

where $\widetilde{\boldsymbol{a}}$ denotes the space-time steering vector of the estimated interference signals. $\Delta\theta$ and Δf represent angular and frequency intervals in $\widetilde{\boldsymbol{\Phi}}$, respectively. It should be noted that the values of $\Delta\theta$ and Δf are less than the error allowance; otherwise, they may suppress the desired signals.

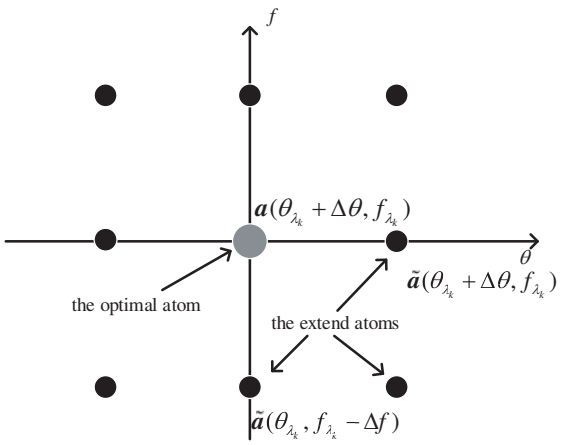

Figure 2. Rectangular AE method of the optimal atom.

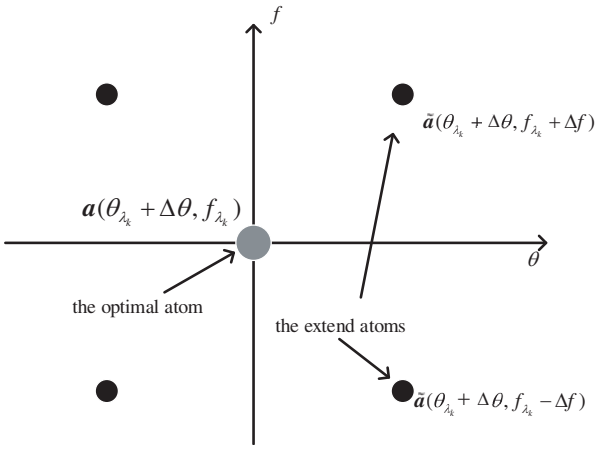

Figure 3. X-shaped AE method of the optimal atom.

Compared with Fig. 2, X-shaped AE method has a negative influence on a smaller number of adjacent atoms. Then, the atomic cluster $\widetilde{\boldsymbol{u}}_{k2}$ can be regarded as the optimal cluster $\widetilde{\boldsymbol{u}}_k$. A new optimal atoms matrix $\widetilde{\boldsymbol{U}}^*$ consisting of the optimal clusters can be expressed as

$$\widetilde{\boldsymbol{U}}^* = [\tilde{\boldsymbol{u}}_1, \tilde{\boldsymbol{u}}_2, \ldots, \tilde{\boldsymbol{u}}_L] \tag{10}$$

where $\widetilde{\boldsymbol{u}}_k$ $(k = 1, 2, \ldots, L)$ is the kth optimal cluster.

3.3. Solution of the Space-Time Optimal Weight Vector

The optimal weight vector $\boldsymbol{w}_{opt}$ with minimum variance distortionless response (MVDR) algorithm can be written as

$$\min_{\boldsymbol{w}} \quad \boldsymbol{w}^{\mathrm{H}}\boldsymbol{R}_x\boldsymbol{w} \quad s.t.\ \boldsymbol{w}^{\mathrm{H}}\boldsymbol{a}(\theta_s, f_s) = 1 \tag{11}$$

where $\boldsymbol{R}_x = \mathbf{E}(\boldsymbol{x}(t)\boldsymbol{x}(t)^{\mathrm{H}})$ stands for the convariance matrix of the received signals.

The optimization problem in Eq. (11) can be solved by Lagrange multiplier method. Then the optimal weight vector $\boldsymbol{w}_{opt}$ can be given by

$$\boldsymbol{w}_{opt} = (\boldsymbol{a}(\theta_s, f_s)^{\mathrm{H}}\boldsymbol{R}_x^{-1}\boldsymbol{a}(\theta_s, f_s))^{-1}\boldsymbol{R}_x^{-1}\boldsymbol{a}(\theta_s, f_s) = \mu\boldsymbol{R}_x^{-1}\boldsymbol{a}(\theta_s, f_s) \tag{12}$$

where $\mu = (\boldsymbol{a}(\theta_s, f_s)^{\mathrm{H}}\boldsymbol{R}_x^{-1}\boldsymbol{a}(\theta_s, f_s))^{-1}$ is a constant. Thus, the optimal weight vector $\boldsymbol{w}_{opt}$ is related to the covariance matrix $\boldsymbol{R}_x$ of received signals. $\boldsymbol{R}_x$ can be formulated as $\boldsymbol{R}_x = \boldsymbol{R}_s + \boldsymbol{R}_j + \boldsymbol{R}_n$ with $\boldsymbol{R}_s$, $\boldsymbol{R}_j$, and $\boldsymbol{R}_n$ denoting the covariance matrix of desired signal, interference signals, and noise, respectively.

Generally, the power of narrow-band compression interference signals is much greater than the noise and the desired signal. Hence, the covariance matrix $\boldsymbol{R}_x$ can be formulated by a block diagonal matrix as

$$\boldsymbol{R}_x \approx \boldsymbol{R}_j + \boldsymbol{R}_n = \boldsymbol{R}_{j+n} = (\sigma^2\boldsymbol{I} + \boldsymbol{A}_j\boldsymbol{R}_j\boldsymbol{A}_j^{\mathrm{H}}) \tag{13}$$

where σ^2 is the power of white Gaussian noise, and $\boldsymbol{I}$ is an $MN \times MN$ identity matrix. $\boldsymbol{R}_j = \mathrm{diag}(\delta_1, \delta_2, \ldots, \delta_L)$ with δ_i denoting the power of the ith interference signal. $\boldsymbol{A}_j = [\boldsymbol{a}(\theta_1, f_1), \boldsymbol{a}(\theta_2, f_2), \ldots, \boldsymbol{a}(\theta_L, f_L)]$ represents the interference signals.

According to matrix inversion lemma, $\boldsymbol{R}_{j+n}^{-1}$ can be written as

$$\boldsymbol{R}_{j+n}^{-1} = \frac{1}{\sigma^2}(\boldsymbol{I} + \sigma^{-2}\boldsymbol{A}_j\boldsymbol{R}_j\boldsymbol{A}_j^{\mathrm{H}})^{-1} = \frac{1}{\sigma^2}\left[\boldsymbol{I} - \boldsymbol{A}_j(\sigma^2\boldsymbol{R}_j^{-1} + \boldsymbol{A}_j^{\mathrm{H}}\boldsymbol{A}_j)^{-1}\boldsymbol{A}_j^{\mathrm{H}}\right] \tag{14}$$

The power of the narrow-band interference signals is much larger than that of noise. Then Eq. (14) can be rewritten as

$$\boldsymbol{R}_{j+n}^{-1} \approx \frac{1}{\sigma^2}\left[\boldsymbol{I} - \boldsymbol{A}_j(\boldsymbol{A}_j^{\mathrm{H}}\boldsymbol{A}_j)^{-1}\boldsymbol{A}_j^{\mathrm{H}}\right] = \frac{1}{\sigma^2}\boldsymbol{P}_{\boldsymbol{A}_j}^{\perp} \tag{15}$$

where $\boldsymbol{P}_{\boldsymbol{A}_j}^{\perp} = \boldsymbol{I} - \boldsymbol{A}_j(\boldsymbol{A}_j^{\mathrm{H}}\boldsymbol{A}_j)^{-1}\boldsymbol{A}_j^{\mathrm{H}}$ stands for the orthogonal projection matrix of the interference signals matrix $\boldsymbol{A}_j$.

Accordingly, the optimal weight vector in Eq. (12) can be rewritten as

$$\boldsymbol{w}_{opt} = \mu\boldsymbol{R}_x^{-1}\boldsymbol{a}(\theta_s, f_s) \approx \mu\boldsymbol{R}_{j+n}^{-1}\boldsymbol{a}(\theta_s, f_s) \approx \frac{\mu}{\sigma^2}\boldsymbol{P}_{\boldsymbol{A}_j}^{\perp}\boldsymbol{a}(\theta_s, f_s) \tag{16}$$

It is evident that the space-time weight vector $\boldsymbol{w}_{opt}$ depends on the orthogonal projection matrix of the interference signals matrix $\boldsymbol{A}_j$ when the angle and frequency of the desired signal are confirmatory. Let the interference signals matrix $\boldsymbol{A}_j$ be expressed by the optimal atoms matrix $\widetilde{\boldsymbol{U}}^*$, that is $\boldsymbol{A}_j = \widetilde{\boldsymbol{U}}^*$. On this basis, the space-time optimal weight vector in Eq. (16) can be solved with the optimal atoms matrix $\widetilde{\boldsymbol{U}}^*$. Then, the space-time optimal weight vector $\boldsymbol{w}_{opt}$ is given by

$$\boldsymbol{w}_{opt} = \frac{\mu}{\sigma^2}\boldsymbol{P}_{\boldsymbol{A}_j}^{\perp}\boldsymbol{a}(\theta_s, f_s) = \frac{\mu}{\sigma^2}\{\boldsymbol{I} - \widetilde{\boldsymbol{U}}^*\left[(\widetilde{\boldsymbol{U}}^*)^{\mathrm{H}}\widetilde{\boldsymbol{U}}^*\right]^{-1}(\widetilde{\boldsymbol{U}}^*)^{\mathrm{H}}\}\boldsymbol{a}(\theta_s, f_s) = \frac{\mu}{\sigma^2}\boldsymbol{P}_{\widetilde{\boldsymbol{U}}^*}^{\perp}\boldsymbol{a}(\theta_s, f_s) \tag{17}$$

where $\boldsymbol{P}_{\widetilde{\boldsymbol{U}}^*}^{\perp} = \boldsymbol{I} - \widetilde{\boldsymbol{U}}^*\left[(\widetilde{\boldsymbol{U}}^*)^{\mathrm{H}}\widetilde{\boldsymbol{U}}^*\right]^{-1}(\widetilde{\boldsymbol{U}}^*)^{\mathrm{H}}$ is the orthogonal projection matrix of interference signals matrix.

The procedure of the proposed algorithm can be summarized as in Table 1.

Table 1. AE-STAP algorithm.

Input : The received signals $\boldsymbol{x}(t)$ and the number of interference signals L
Output : Space-time weight vector $\boldsymbol{w}_{opt}$
Procedure
Step 1. Construct space-time dictionary $\boldsymbol{\Phi}$ and formulate optimisation problem according to (7).
Step 2. Obtain the optimal atoms matrix $\widetilde{\boldsymbol{\Phi}}$ and support set Λ by OMP algorithm.
Step 3. Estimate the interference subspace with AE methods according to (8)–(10).
Step 4. Calculate the orthogonal projection matrix $\boldsymbol{P}_{\widetilde{\boldsymbol{U}}^*}^{\perp}$ of the interference signals matrix: $\boldsymbol{P}_{\widetilde{\boldsymbol{U}}^*}^{\perp} = \boldsymbol{I} - \widetilde{\boldsymbol{U}}^*\left[(\widetilde{\boldsymbol{U}}^*)^{\mathrm{H}}\widetilde{\boldsymbol{U}}^*\right]^{-1}(\widetilde{\boldsymbol{U}}^*)^{\mathrm{H}}$.
Step 5. Calculate the optimal weight vector: $\boldsymbol{w}_{opt} = \frac{\mu}{\sigma^2}\boldsymbol{P}_{\widetilde{\boldsymbol{U}}^*}^{\perp}\boldsymbol{a}(\theta_s, f_s)$.

4. SIMULATION RESULTS

In this section, several simulations are constructed to evaluate the performance of the proposed method. Meanwhile, the proposed algorithm is compared with MVDR algorithm [19], PI algorothm [21], CS-SF algorithm [20], and OMP-ISRP algorithm [22].

Assume that the ULA is composed of 8 antennas with equally spaced $d = 0.098$m. Each antenna element is equally spaced with 7 delay taps. Assume that the desired signal whose DOA $\theta = 0^\circ$ and frequency $f = 1.575$ GHz (the normalized frequency is 1 GHZ). There are three narrow-band interference signals whose DOAs and normalized frequencies are $(-60^\circ, 0.9)$, $(20^\circ, 1.1)$, and $(50^\circ, 1.2)$, respectively. The input signal-to-noise ratio (SNR) is set to -20 dB. The noise is a zero-mean white Gaussian noise with power $\sigma^2 = 1$. For the interval unit of dictionary, the angular interval is fixed as 1°, and the normalized frequency interval is set as 0.01.

Figure 4 illustrates the matching degree between the presupposed interference signals and the optimal atoms in the space-time dictionary. The matching degree is determined by the vertical projection length in the direction of each optimal atom. As shown in Fig. 4, there are three peaks located at $(-60^\circ, 0.9)$, $(19^\circ, 1.09)$, and $(51^\circ, 1.22)$, respectively. The DOAs and normalized frequencies of peaks do not accord with the presupposed interference signals. Two main factors are considered. Firstly, matching bias may be caused by strong correlation of adjacent atoms in the space-time dictionary. Secondly, the noises affect the degree of matching between the interference signals and the atoms for

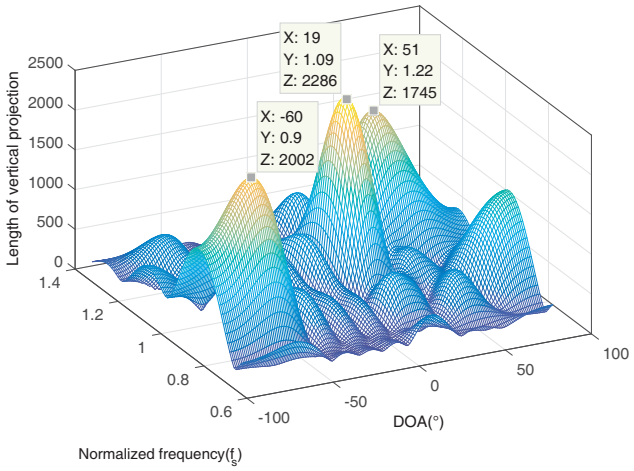

Figure 4. Matching degree for the received signals versus the dictionary atoms(with the noises).

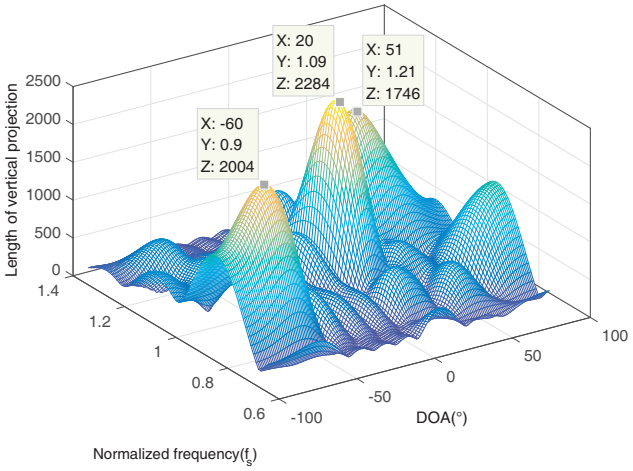

Figure 5. Matching degree for the received signals (without the noises) versus the dictionary atoms.

the space-time dictionary. Fig. 5 illustrates the matching degree between the presupposed interference signals and the space-time optimal atoms in the case without the noises. As shown in Fig. 5, the simulation results are similar to the results in Fig. 4. The above situations occur because the noises may have a negative influence on the matching bias, but it is not the main factor. Matching bias is mainly caused by strong correlation of adjacent atoms in the space-time dictionary. Therefore, OMP algorithm can just identify the optimal atoms approximately.

Figures 6 and 7 show the space-frequency response and the contour map of AE-STAP algorithm when the optimal atoms are extended with the rectangular AE method. As shown in Fig. 6, three nullings are formed at the DOAs of the interference signals, and a distortionless response is maintained for the desired signal. In order to show the range of the formed nullings distinctly, the contours of AE-STAP algorithm with the rectangular extension method is plotted in Fig. 7. It is evident that there are three interference signals located at around $(-60°, 0.9)$, $(20°, 1.1)$, and $(50°, 1.2)$, respectively. In addition, the nullings are wide, which have negative influences on the gain of the signals near interferences. When the DOAs and frequencies of the interference signals are close to the desired

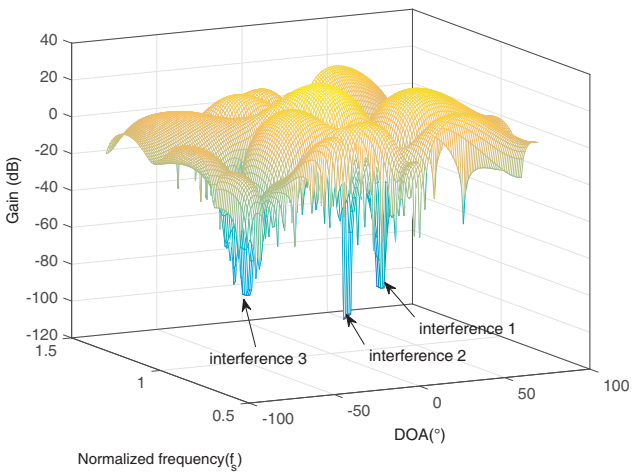

Figure 6. Space-frequency response of AE-STAP algorithm (rectangle).

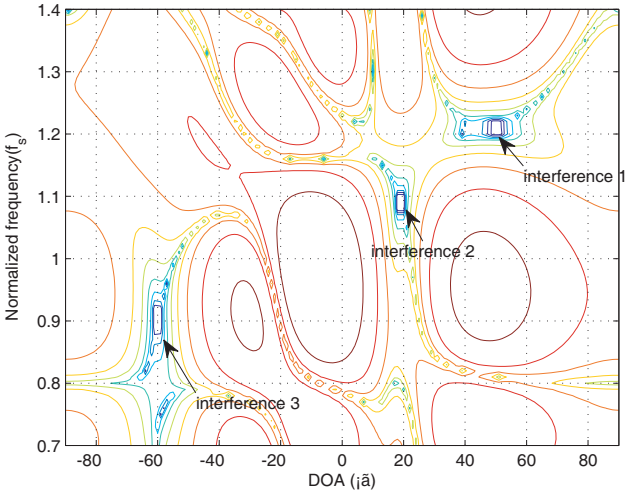

Figure 7. Contour map of AE-STAP algorithm space-frequency response (rectangle).

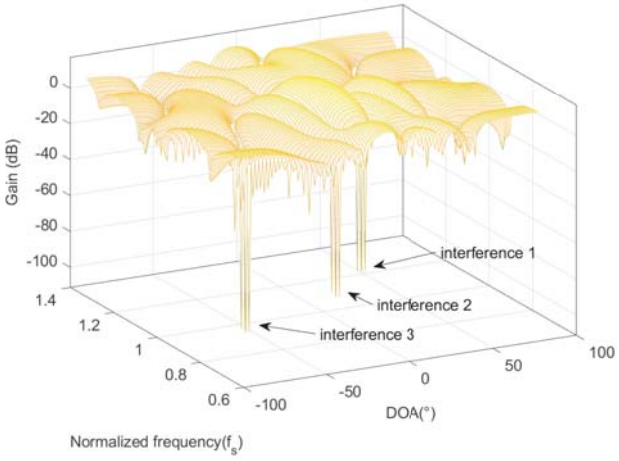

Figure 8. Space-frequency response of AE-STAP algorithm (X-shaped).

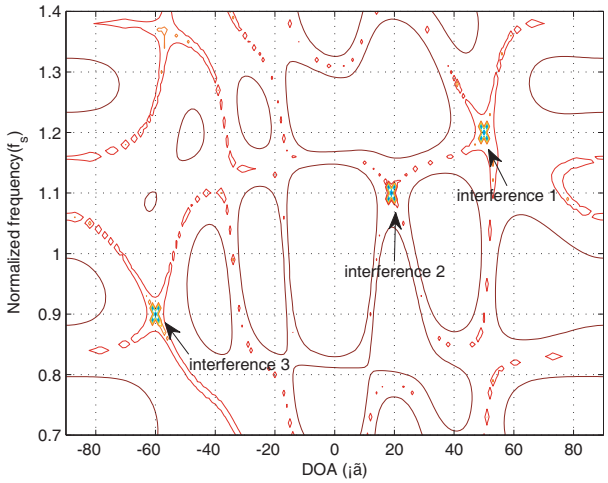

Figure 9. Contour map of AE-STAP algorithm space-frequency response (X-shaped).

signal, it will cause distortion of the desired signal.

Figures 8 and 9 show the space-frequency response and the contour map of AE-STAP algorithm with the X-shaped AE method. It can be seen that the proposed algorithm can also form nullings in the corresponding DOAs and frequencies of the interference signals. Compared with the rectangular AE method, AE-STAP algorithm with the X-shaped AE method to form deeper nullings and the points near nullings are less negative affected. The anti-jamming performance is better than the rectangular AE method. Therefore, in the subsequent simulation experiments, the optimal AE mode is the X-shaped AE method.

To further verify the effectiveness of AE-STAP algorithm, the output SINRs under different DOAs of an interference signal are simulated, and the simulation results are shown in Fig. 10. In this simulation, the angles of the first interference signal and second interference signal are set to $-60°$ and $50°$, respectively. The DOA of the third interference signal is traversed from $-90°$ to $90°$. The number of snapshots is set to 64. It is evident that the proposed method achieves higher output SINRs than other methods. This is due to the estimation errors of signal covariance matrix for traditional

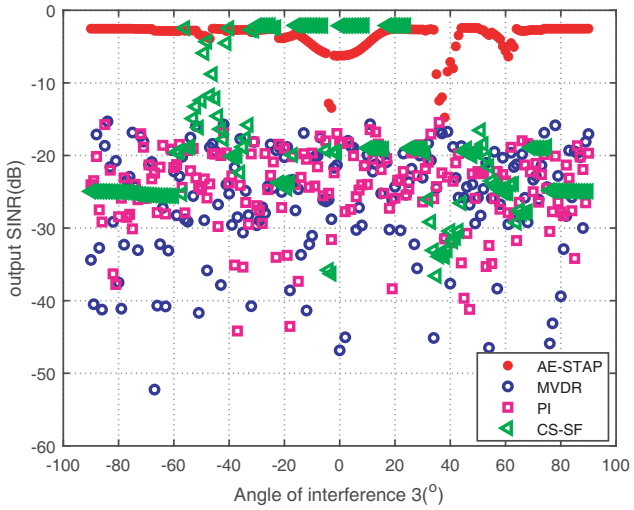

Figure 10. Output SINR versus the angle of interference 3.

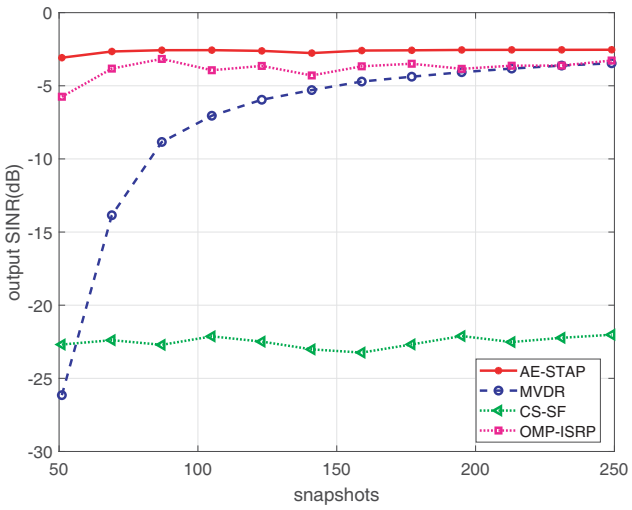

Figure 11. Output SINR versus the number of snapshots.

MVDR and PI anti-jamming algorithms when there are fewer snapshots. CS-SF method can achieve output SINRs the same level as the proposed algorithm in certain angles. However, CS-SF method has poor performance in other angles, which is caused by the optimal atomic estimation error in the sparse recovery process. The proposed algorithm extends the optimal atoms, which can estimate the interference subspace more accurately. Therefore, the proposed method achieves significantly higher SINRs than CS-SF and MVDR methods under a small number of snapshots. Besides, AE-STAP method is an interference nulling algorithm so that it can form deep nullings, which does not need the power of the interference signals and only uses the DOAs and frequencies of the interference signals.

As shown in Fig. 11, the anti-jamming performances of each method are compared in terms of the output SINRs under different numbers of snapshots. The proposed method still achieves stable output SINRs even when the number of snapshots is fewer than 55. With the number of snapshots growing, it can be seen that the output SINRs of the proposed algorithm are similar to MVDR and OMP-ISRP algorithms. And CS-SF algorithm has lower output SINRs than other methods. It means that the proposed algorithm has better anti-jamming performance than the other methods even under a small number of snapshots.

5. CONCLUSION

In this paper, an effective AE-STAP algorithm is proposed to solve the off-grid SR-STAP problem even in the case of low sample support. Based on the sparsity of received signals, OMP algorithm is used to effectively select more appropriate atoms that are matched with interference signals. Then, an AE method is proposed to reduce the estimation bias. On this basis, the interference subspace is constructed. Finally, the space-time optimal steering vector is calculated with the orthogonal projection matrix of interference subspace. Simulation results demonstrate that the proposed algorithm can achieve superior interference suppression performance.

ACKNOWLEDGMENT

This work was supported by the National Natural Science Foundation of China (Grant No. 61971117), by the Natural Scienence Foundation of Hebei province (Grant No. F2020501007) and by the Fundamental Research Funds for the Central Universities (Grant No. N172302002).

REFERENCES

1. Zhu, Z. S. and C. Li, "Study on real-time identification of GNSS multipath errors and its application," *Aerospace Science and Technology*, Vol. 52, 215–223, 2016.
2. Xie, F., R. Sun, G. Kang, et al., "A jamming tolerant BeiDou combined B1/B2 vector tracking algorithm for ultra-tightly coupled GNSS/INS systems," *Aerospace Science and Technology*, Vol. 70, 265–276, 2017.
3. Melvin, W. L., "Space-time adaptive radar performance in heterogeneous clutter," *IEEE Trans. Aerosp. Electron. Syst*, vol. 36,No. 2, 621–633, 2000.
4. Wang, Y., Y. Peng, and Z. Bao, "Space-time adaptive processing for airborne radar with various array orientation," *IEE Radar, Son. Navig*, Vol. 144, No. 6, 330–340, 1997.
5. Wang, H. and L. Cai, "On adaptive spatial-temporal processing for airborne surveillance radar systems," *IEEE Trans. Aerosp. Electron. Syst*, Vol. 30, No. 3, 660–670, 1994.
6. Wang, Y. L., J. W. Chen, Z. Bao, et al., "Robust space-time adaptive processing for airborne radar in nonhomogeneous clutter environments," *IEEE Trans. Aerosp. Electron. Syst*, Vol. 39, No. 1, 70–81, 2003.
7. Wang, X. Y., Z. C. Yang, and R. C. de Lamare, "Robust two-stage reduced-dimension sparsity-aware STAP for airborne radar with coprime arrays," *IEEE Transactions On Signal Processing*, Vol. 68, 81–96, 2020.
8. Haimovich, A. M., "An eigencanceler: Adaptive radar by eigenanalysis methods," *IEEE Trans. Aerosp. Electron. Syst*, Vol. 32, No. 2, 532–542, 1996.

9. Goldstein, J. S. and I. S. Reed, "Reduced rank adaptive filtering," *IEEE Trans. Signal Process*, Vol. 45, No. 2, 492–496, 1997.
10. Myrick, W. L., M. D. Zoltowski, and J. S. Goldstein, "Low-sample performance of reduced-rank power minimization based jammer suppression for GPS," *IEEE Sixth International Symposium on Spread Spectrum Techniques and Applications*, Vol. 1, 91–97, 2000.
11. Jeon, H., Y. Chung, W. Chung, et al., "Clutter covariance matrix estimation using weight vectors in knowledge-aided STAP," *Electronics Letters*, Vol. 53, No. 8, 560–562, 2017.
12. Wang, Z., W. Xie, K. Duan, et al., "Clutter suppression algorithm based on fast converging sparse Bayesian learning for airborne radar," *Signal Process*, Vol. 130, 159–168, 2017.
13. Han, S., C. Fan, and X. Huang, "A novel STAP based on spectrum-aided reduced-dimension clutter sparse recovery," *IEEE Geosci. Remote Sens. Lett*, Vol. 14, No. 2, 213–217, 2017.
14. Duan, K. Q., W. J. Liu, G. Q. Duan, et al., "Off-grid effects mitigation exploiting knowledge of the clutter ridge for sparse recovery STAP," *IET Radar, Sonar & Navigation*, Vol. 12, 557–564, 2018.
15. Dai, J., X. Bao, W. Xu, et al., "Root sparse bayesian learning for off-grid DOA estimation," *IEEE Signal Process. Lett.*, Vol. 24, No. 1, 46–50, 2017.
16. Wen, C., X. Xie, and G. Shi, "Off-grid DOA estimation under nonuniform noise via variational Sparse Bayesian learning," *Signal Processing*, Vol. 137, 69–79, 2017.
17. Bai, G., R. Tao, J. Zhao, et al., "Parameter-searched OMP method for eliminating basis mismatch in space-time spectrum estimation," *Signal Processing*, Vol. 138, 11–15, 2017.
18. Li, Z., Y. Zhang, Q. Gao, et al., "Off-grid STAP algorithm based on local search orthogonal matching pursuit," *2019 IEEE 4th International Conference on Signal and Image Processing*, 187–191, 2019.
19. Capon, J., "High-resolution frequency-wavenumber spectrum analysis," *Proceedings of the IEEE*, Vol. 57, No. 8, 1408–1418, 1969.
20. Liu, F. L., L. Liu, et al., "CS-SFD algorithm for GNSS anti-jamming receivers," *Progress In Electromagnetics Research M*, Vol. 79, 91–100, 2019.
21. Compton, R. T. and J. R. Russer, "The power-inversion adaptive array: concept and performance," *IEEE Transactions on Aerospace and Electronic Systems*, Vol. 15, No. 6, 803–815, 1979.
22. Wang, W., Q. Du, R. Wu, et al., "Interference suppression with flat gain constraint for satellite navigation systems," *Radar Sonar & Navigation Iet*, Vol. 9, No. 7, 852–856, 2015.